Release timing and duration control the fate of photolytic compounds in stream-1 2 hyporheic systems 3 4 This manuscript has been submitted for publication in Environmental Science & Technology. Please 5 note that this version has not undergone peer review and has not been formally accepted for 6 publication. Subsequent version of this manuscript may have slightly different content. If accepted, 7 the final version of this manuscript will be available via the Peer Reviewed Publication DOI link on 8 the right-hand side of this webpage. Please contact the corresponding author with any questions or 9 concerns. 10 Hixson, Jase L.1* 11 Ward, Adam S. 1 12 McConville, Megan B.² 13 Remucal, Christina K. ^{2,3} 14 15 ¹O'Neill School of Public and Environmental Affairs, Indiana University, Bloomington, 16 17 Indiana, USA ² Environmental Chemistry and Technology Program, University of Wisconsin – Madison, 18 19 Madison, Wisconsin, USA. ³ Department of Civil and Environmental Engineering, University of Wisconsin – Madison, 20 Madison, Wisconsin, USA 21 22 Correspondence To: 23 24 Jase L. Hixson 25 O'Neill School of Public and Environmental Affairs 26 Indiana University 450A MSB-II, Bloomington, IN 47405 27 jhixson@indiana.edu 28 29

Abstract

31

49 50

51

52

53

54

55

56

57

58 59

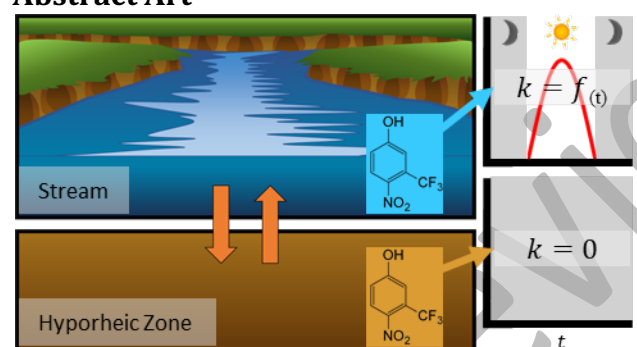
60

61 62

63 64

Predicting environmental fate requires an understanding of the underlying. 32 spatiotemporally variable interaction of transport and transformation processes. 33 Photolytic compounds, for example, interact with both time-variable photolysis and the 34 perennially dark hyporheic zone, generating potentially unexpected dynamics that arise 35 from time-variable reactivity. This interaction has been found to significantly impact 36 37 environmental fate but is commonly oversimplified in predictive models. Our primary objective was to explore how time-variable photolysis and hyporheic storage interact 38 39 across a range of photolysis rates to control the fate and transport of photolytic solutes in 40 stream-hyporheic systems. In this study, we simulated variable release timing and durations of photolytic compounds spanning half-lives of 2.8 minutes to 908 hours. To 41 contextualize these results, we interpret results 3-trifluoromethyl-4-nitrophenol (TFM), as 42 its photolysis rate is controlled by environmental conditions and is known to vary by 43 44 several orders of magnitude. Ultimately, we found the environmental fate and transport of photolytic compounds is highly variable as a function of release timing, which controls 45 46 when, where, and for how long solute is stored in the hyporheic zone or exposed to inchannel photolysis. This knowledge can be used to improve predictions for photolytic 47 48 compounds or assess potential impacts for an anticipated discharge or treatment.

Abstract Art



Keywords

- 1. Photolysis
- 2. Diel
- 3. Environmental transport and fate
- 4. Hyporheic
- 5. Emerging contaminant
- 6. 3-trifluoromethyl-4-nitrophenol

Synopsis

Release timing of photolytic compounds interacts with transport and time-variable transformation processes to control exposure and persistence in stream-hyporheic systems.

1. Introduction

65

66

67

68

69

70

71

72

73

74

75

76

77

78

79

80

81

82

The environmental fate of organic chemicals released into surface waters is controlled by intrinsic properties of the compound, spatiotemporally variable drivers of transformation, and transport processes.¹ Controlling for differential reactivity of compounds to spatiotemporally variable reactivity in natural systems is necessary to advance our ability to predict their fate and transport.² For example, solar radiation and temperature are commonly accounted for as dynamic drivers of reaction rates at both seasonal^{3,4} and diurnal timescales, including impacts on dissolved oxygen, dissolved organic carbon. nitrogen species, carbonate species, algae, and metals.⁵⁻¹² Sub-diel timescales also exhibit the time-variability in response to forcing (e.g., cloud cover blocking solar radiation, predictable dynamics of sunrise and sunset), but are often overlooked or oversimplified in the name of parsimony. 13,14 While many diel-varying processes have been studied individually, their interaction with reactive transport processes, such as temporary storage in the hyporheic zone where photolysis cannot occur, are seldom studied. 15,16 The interaction of diurnal variation in solar radiation with reactivity is known to be important for environment transport and fate in riparian ecosystems, having been considered in a limited number of empirical studies.^{5,17–20} Here, we systematically study how release timing and duration interact with sub-diel variation in reactivity to control the transport and fate of photolytic compounds in river corridors.

84

85

86

87

83

Physical transport and reactive processes have been widely studied as individual controls on photolytic compounds, with a limited number of studies incorporating interactions between the two.^{15,21–23} For example, in the case of a stream at steady flow conditions, the

interaction of time-variable photolysis with the transient storage of photolytic compounds in the perennially dark hyporheic zones is critical to forecasting environmental fate of photolytic compounds. He hyporheic zone has been found to shield hyporheic water from changes in solar radiation 16,24 and air temperature, 25,26 few studies have incorporated the time-variability of reactive processes with storage in the hyporheic zone. It is well documented that hyporheic storage processes vary under short timescales around perturbations such as changes in discharge from storm events. Still other applications account for time-variable photolysis rates, but fail to consider transport dynamics that account for temporary storage within permanently dark hyporheic zones. Thus, advancing our predictive understanding of the environmental fate of photolytic compounds requires an improved integration of stream-hyporheic exchange with time-variable transformation processes.

To motivate our study, we consider the transport and fate of 3-trifluoromethyl-4-nitrophenol (TFM; used to control invasive sea lamprey in the Great Lakes) as a representative case to study. TFM is a photolytic compound that is fatal to invasive sea lamprey larvae that spend the early years of their lifecycle in the hyporheic zone.

Application of TFM occurs in tributaries of the Great Lakes on a 1-to-5-year rotation to control sea lamprey populations. Although sea lamprey are particularly sensitive to TFM, chemical application may precede amphibian deaths, decreased algal productivity, and loss of coordination in birds. Major losses of TFM that are accounted for in planning treatments include losses due to in-stream photolysis and dilution due to transport into hyporheic zones. TFM photolysis in natural systems occurs primarily through direct,

rather than indirect, photolysis.³⁸ Additionally, reach-scale effective TFM photolysis rates will vary as a function of water column depth, pH, incident solar radiation (itself a function of location and time of year), and the in-stream concentration of TFM. Taken together, these controls cause effective decay rates realized during treatments to span several orders of magnitude.³⁹ Thus, TFM provides a useful case study given its well-known reactive pathways, widespread application to stream-hyporheic systems in the Great Lakes Basin, and potential risk to ecosystem and human health.

The overarching goal of this study is to advance our understanding of how time-variable reactivity and hyporheic exchange interact to control the fate and transport of photolytic solutes in stream-hyporheic systems. Specifically, we seek to characterize changes in exposure to and persistence of photolytic compounds as a function of release timing and duration in stream-hyporheic systems. To achieve these objectives, we conducted a series of numerical experiments for photolytic compounds in an idealized headwater stream. While we interpret these results in the context TFM applications in the tributaries of the Great Lakes, we also model the fate of a more photolabile and less photolabile compound (i.e., ketoprofen and carbamazepine, respectively) to more completely explore the range of loss rates expected for polar organic compounds. By assessing a range of light-sensitive organic chemicals our findings are generalizable to other compounds subject to photolysis in stream-hyporheic systems.

2. Methods

2.1 Simulation of compound release timing and duration

We implement here a model to simulate transport and transformation of photolytic compounds in stream hyporheic systems, following Ward et al., 2015.40 Briefly, the model simulates advection, dispersion, first-order decay proportional to a half-sinusoid representing solar radiation occurring from 06:00-18:00, and transient storage in a wellmixed hyporheic zone with an exponential residence time distribution.^{21,41} We tested peak photolysis rates to represent the maximum ($k_2 = 5.56 \times 10^{-5} \,\mathrm{s}^{-1}$), median ($k_3 = 7.44 \times 10^{-6} \,\mathrm{s}^{-1}$). and minimum (k_4 =4.98×10⁻⁷ s⁻¹) rates for TFM reported in Great Lakes tributaries.³⁹ To expand our study beyond consideration of only TFM, we selected an additional compound that is highly photoreactive and an additional compound that is more resistant to photolysis: (1) ketoprofen, an anti-inflammatory drug, with a peak photolysis rate of k_1 =4.18×10⁻³ s⁻¹ and (2) carbamazepine, an anticonvulsant, with a photolysis rate of k_5 =2.12×10⁻⁷ s⁻¹.42,43 Reaction rate subscripts are ordered from fastest (k_1) to slowest (k_5) to aid in interpretation of results. The model assumes a stream at steady baseflow, with fixed stream geometry, hyporheic geometry, dispersion, exchange rate, and spatial and temporal discretization at the values used by Ward et al. (2015). In all cases, we simulated an 80-km total length of stream to ensure downstream boundary were isolated from the model behavior immediately downstream of the injection.

151

152

153

154

155

156

134

135

136

137

138

139

140

141

142

143

144

145

146

147

148

149

150

To assess the impact of release timing and duration on environmental fate, we simulated a series of releases beginning every hour of the day and varied release durations from 1 to 24 hours in one-hour increments, plus 36 and 48 hr durations (totaling 624 simulations per k; 3,120 overall). In-stream persistence was calculated as the distance along the stream until the peak concentration was reduced by 50% of the input concentration (90% and 99%).

were also calculated). We also tabulated the total mass flux of the parent compound at each location along the reach. Finally, we calculated the total time that the stream concentration is greater than 10% of the input concentration at a given location to represent a combined concentration and duration criteria like that used to confirm successful TFM treatment. For time above treatment concentration, we selected a point 6-km downstream of the injection to compare mass flux (the median treatment length for small tributaries in the Great Lakes Basin). The simulated treatment concentration (3.6 mg L⁻¹) represents the mean concentration applied during the 2015 seasons³⁸.

2.2 TFM treatment of Great Lakes tributaries

TFM is intentionally released in more than 100 Great Lakes tributaries per year by the U.S. Fish and Wildlife Service and Fisheries and Oceans Canada to control invasive sea lamprey populations. The standard application of TFM involves a constant-rate release typically beginning in the morning and continuing through the day.⁴⁴ Effective treatment is defined as a concentration 1.1-1.4 times greater than the minimum lethal concentration for sea lamprey for a duration of 12 hours in the stream. This is assumed to also represent effective treatment of the hyporheic zone where lamprey spend a portion of their lifecycle^{39,45,46}. We simulated 12 hr constant-rate releases beginning at 06:00 as representative of this strategy. Based on the targeted minimum lethal concentration reported by the U.S. Fish and Wildlife Service and Fisheries and Oceans Canada, from 1961-2016, the minimum targeted concentration for an effective treatment was 0.3 mg L⁻¹. Therefore, treatment is reasonably approximated as the stream concentration at or above 10% (or 0.36 mg L⁻¹) of the average well-mixed concentration at the treatment location of

36 mg/L. In practice, dosing rates are adjusted in the field to achieve concentration thresholds in each system based on monitoring during treatment. Additionally, we interpret the places and times where concentrations are above 50% of the input concentration as potential locations of over-treatment, with anomalously high exposure to TFM. The location and duration of concentrations above 10% of the input concentration in both the stream and hyporheic zone are interpreted to represent effective treatment.

3. Results and Discussion

3.1 How do release timing and duration control in-stream transport?

3.1.1. Release timing controls persistence for releases less than 24 hour in duration In-stream persistence had a maximum distance of 41 km (Fig. 1). Persistence varies from <1 km to 22 km (k_1) and from <1 km to 30 km (k_2), depending on release timing (Fig. 1a-b). Distances to achieve 90% reduction in peak concentration also varied with release timing for the fastest rate (k_1), ranging from <1 km to 24 km, while k_2 and slower were insensitive to release timing (90% reduction occurring around 45 km for k_2 ; Fig. 1b). Distances to achieve 99% reduction for k_1 vary from about 1 to 25 km, with maximum persistence occurring for the injection at 16:00). The slowest three rates (k_3 , k_4 , k_5) each persisted for about 40 km for nearly every release time (Table 1; Fig. 1c-e). Distances to achieve both 90% and 99% reduction in peak concentration were 80 km (maximum simulated stream reach), regardless of release time for k_2 through k_5 (Fig. 1b-e). Across all reaction rates, minimum persistence occurs for the injection beginning at 12:00, when photolysis is at its

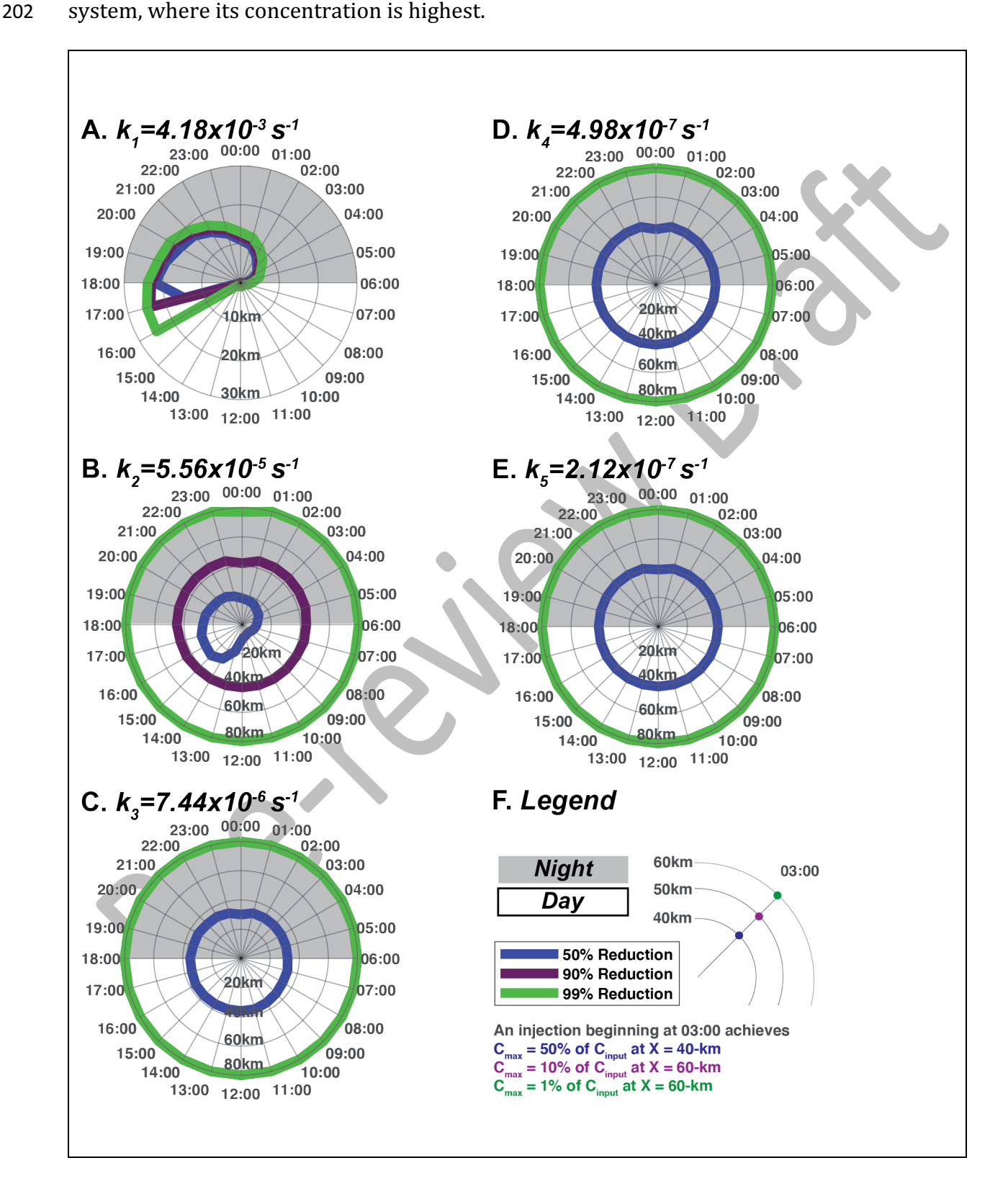


Figure 1. Distance until peak stream concentration drops to 50% (blue), 90% (purple), and 99% (green) input concentration for varying photolysis rates simulated for 1 hour releases beginning every hour of the day. The radius from center corresponds to downstream distance, and radial lines indicate the start time for simulated releases. Photolysis rates were selected based on the analog compounds ketoprofen (a), TFM (b-d), and Carbamazepine (e), ordered from fasted to slowest (top to bottom).

Table 1. Summary of ranges observed for each photolysis rate for each metric explored in this study.

Metric	k_1	k_2	k ₃	k ₄	k_5
Photolysis rate (s-1)	4.18×10 ⁻³	5.56×10-5	7.44×10-6	4.98×10 ⁻⁷	2.12×10 ⁻⁷
Analog Chemical	Ketoprofen	TFM _{max}	TFM _{med}	TFM _{min}	Carbamazepine
Maximum persistence (km)	22	30	36	41	41
Minimum persistence (km)	<1	7	30	38	39
Maximum mass at 6km (% of input)	35.52%	44.73%	45.42%	45.53%	45.56%
Minimum mass at 6km (% of input)	0.21%	31.04%	43.22%	45.00%	45.07%
Release time for max. persistence (hr)	18:00	12:00	Insensitive	Insensitive	Insensitive
Release time for min. persistence (hr)	05:00	00:00	Insensitive	Insensitive	Insensitive

Persistence in the stream is maximized when mass is injected into the system immediately at or after the end of the photoperiod (sunset). For example, the maximum in-stream persistence for k_1 occurred for the injection beginning at 18:00, immediately after sunset (Fig. 1a). The result of mass entering coincident with sunset is that the mass is advected downstream for the 12 hr (i.e., from 18:00 to 06:00) with no photolysis occurring, exposing the longest possible reach to high concentrations. In our study system, the effects of longitudinal dispersion and hyporheic dilution on the solute concentrations are minimal

compared to photolysis for k_1 and k_2 as evidenced by the gradually decreasing persistence observed for releases between 18:00 and 06:00, compared to the rapidly decreasing, and minimal persistence observed between 06:00 and 18:00 (Fig. 1a-b). In contrast, longitudinal dispersion and hyporheic dilution are comparable to photolysis for k_{3-5} , as evidenced by the comparable persistence independent of release timing (Fig. 1c-e). As release durations increase, the release time for maximum persistence becomes systematically earlier for the fastest photolysis rates (Fig. 2a-b). This is in good agreement with the interpretation of timing, where persistence is controlled by mass that enters the system just after sunset. For example, maximum persistence for k_1 occurs for injections beginning at 18:00, the end of the photoperiod (Fig. 2a). Additionally, maximum persistence occurs for a 2 hr duration starting at 17:00 (1 hr before the end of photolysis), a 3 hr duration starting at 16:00, and so forth (Fig. 2a). Again, the timing of the last mass entering the system is key to the observed behavior, rather than the timing of when the release begins. This pattern is consistent for compounds with faster photolysis rates (i.e., k_{1-2}). In contrast, compounds with slower rates (k_{3-5}) are broadly insensitive to release timing (Fig. 2c-e). For these compounds, photolysis becomes minimally important and persistence scales directly with release duration.

215

216

217

218

219

220

221

222

223

224

225

226

227

228

229

230

231

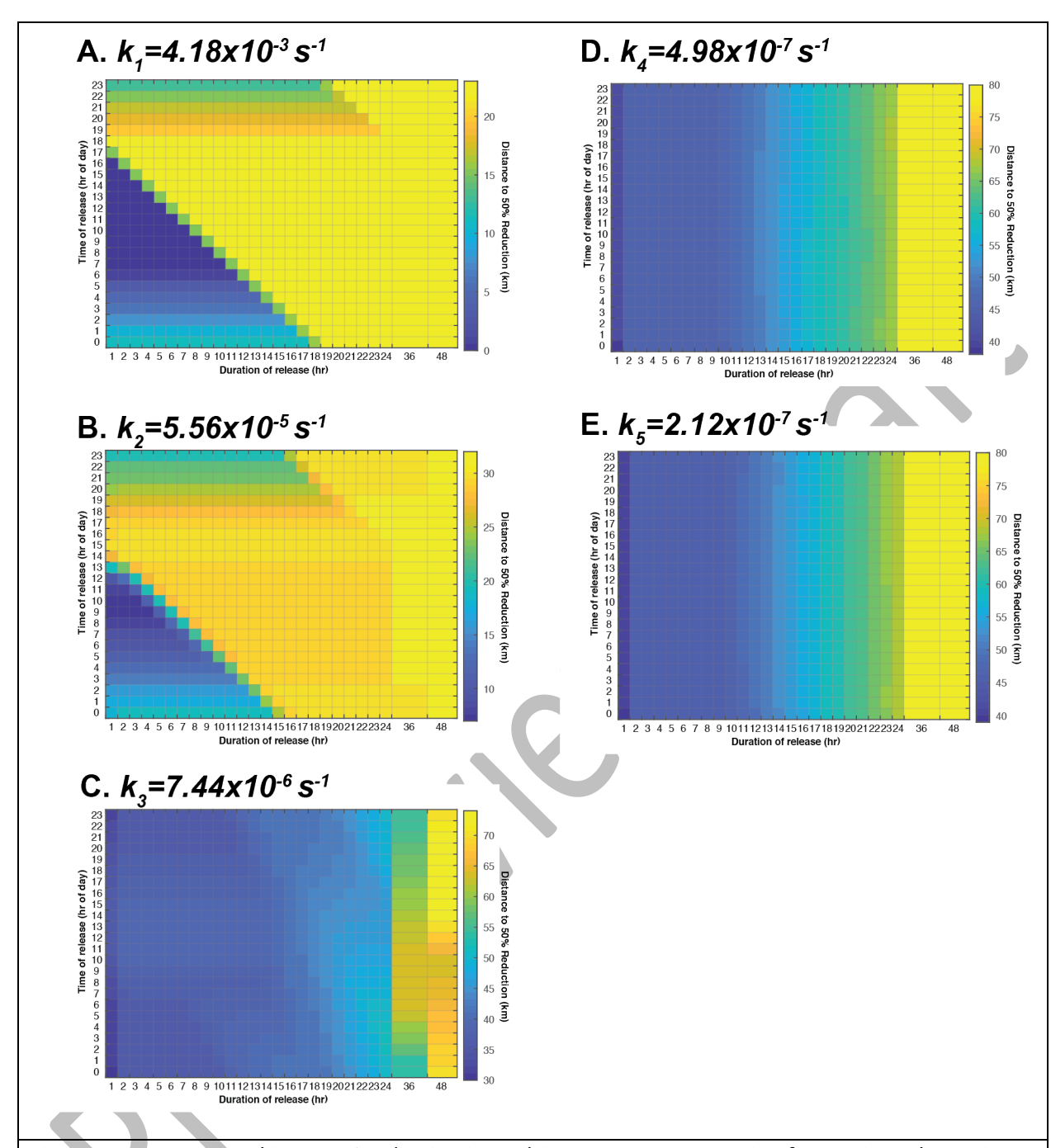


Figure 2. Distance to achieve 50% reduction in peak in-stream concentration for varying release times, durations, and photolysis rates. For each photolysis rate, releases were simulated every hour of the day (y-axis), for release durations of 1-24, 36, and 48 hours (x-axis). The color of each cell corresponds to the along-stream distance to achieve 50% removal of the input concentration for each injection.

For compounds with rapid reaction rates (k_{1-2}) , maximum persistence across all simulations of varying release timing and duration was between 25-33 km. As release duration increased, a larger range of release times result in a downstream persistence greater than 30 km because multiple combinations of starting time and duration result in mass being released at sunset (Fig. 2). As release durations become longer than one day, there is little variation as a function of release timing because there is always mass entering the system at sunset (18:00). In contrast, persistence is always greater than 30 km for compounds with k_{3-5} . In these cases, removal via photolysis is slow enough that every combination of release timing and duration results in less than 50% reductions at the end of one photoperiod. Thus, relatively high concentrations always advect for 12 hours of darkness regardless of timing or duration of chemical addition for k_{3-5} .

Photolysis at rates k_1 and k_2 remove mass faster than it is ever returned to the stream from the hyporheic zone (i.e., a net removal from water column for injections during photoperiods). However, the inverse is true for k_{3-5} , where a net gain of mass by the water column can occur during the photoperiod. For k_{3-5} , as the release duration increases and photolysis remains a minimal removal mechanism, the hyporheic zone begins to saturate with TFM. This ultimately causes increased persistence of the chemical in the downstream direction, extending well beyond the 80-km study reach to achieve even 50% removal.

Depending upon release timing, both short- and long-duration releases can result in equal persistence and equally high concentrations at downstream locations. Persistence of a short (1-2 hr) release can be as great as the persistence of a 24-48 hr release for k_1 and k_2

(Fig. 2a-b). For example, for k_1 both a 1 hr and 24 hr release at 18:00 persists for 22 km downstream because the 12-hr of nighttime advection dominates the response. However, less variability to release timing was observed in slower photolysis rates (k_{3-5}), and release duration dominated persistence. For k_{3-5} , durations ranging between 2-10 hr resulted in the same persistence, regardless of release timing. The insensitivity to release timing can also be observed across every photolysis rate, mass added to the system (release duration), and removal via photolysis approach steady state. For rapid photolysis rates (k_{1-2}), longer release durations are required to approach steady state, while slow photolysis rates approach steady state at shorter release durations.

3.1.2 Spatial and temporal variation as a function of release timing and duration Release timing and duration interact with transport and transformation to yield highly variable exposure (i.e., the time-integrated total mass passing a given spatial location) along the stream. For 1 hr injections, release timing leads to three orders of magnitude in variation for mass exposure for k_1 (Fig. 3a, vertical range at any x-coordinate). For k_2 , exposure varies by up to a factor of 2 for 1 hr injections (Fig. 3b), while variation in exposure for $k_{3.5}$ is nearly identical regardless of release time (Fig. 3c-e). The greatest variability in exposure for 1 hr releases represents the difference between injections occurring at 18:00 (12 hours of transport prior to photolysis) and 12:00 (immediate photolysis at the maximum rate). For 12 hr releases, reduced sensitivity to release timing manifests as a smaller range in total mass exposure, with a range of two orders of magnitude variation for k_1 (Fig. 3a), three-fold variation for k_2 (Fig. 3b), and minimal

variation for k_{3-5} (Fig. 3c-e). The maximum range for 12 hr releases occurs between the 15:00 release and the 03:00 release. Taken together, these results indicate that exposure varies predictably as a function of both system and chemical compound properties, but can be predicted.

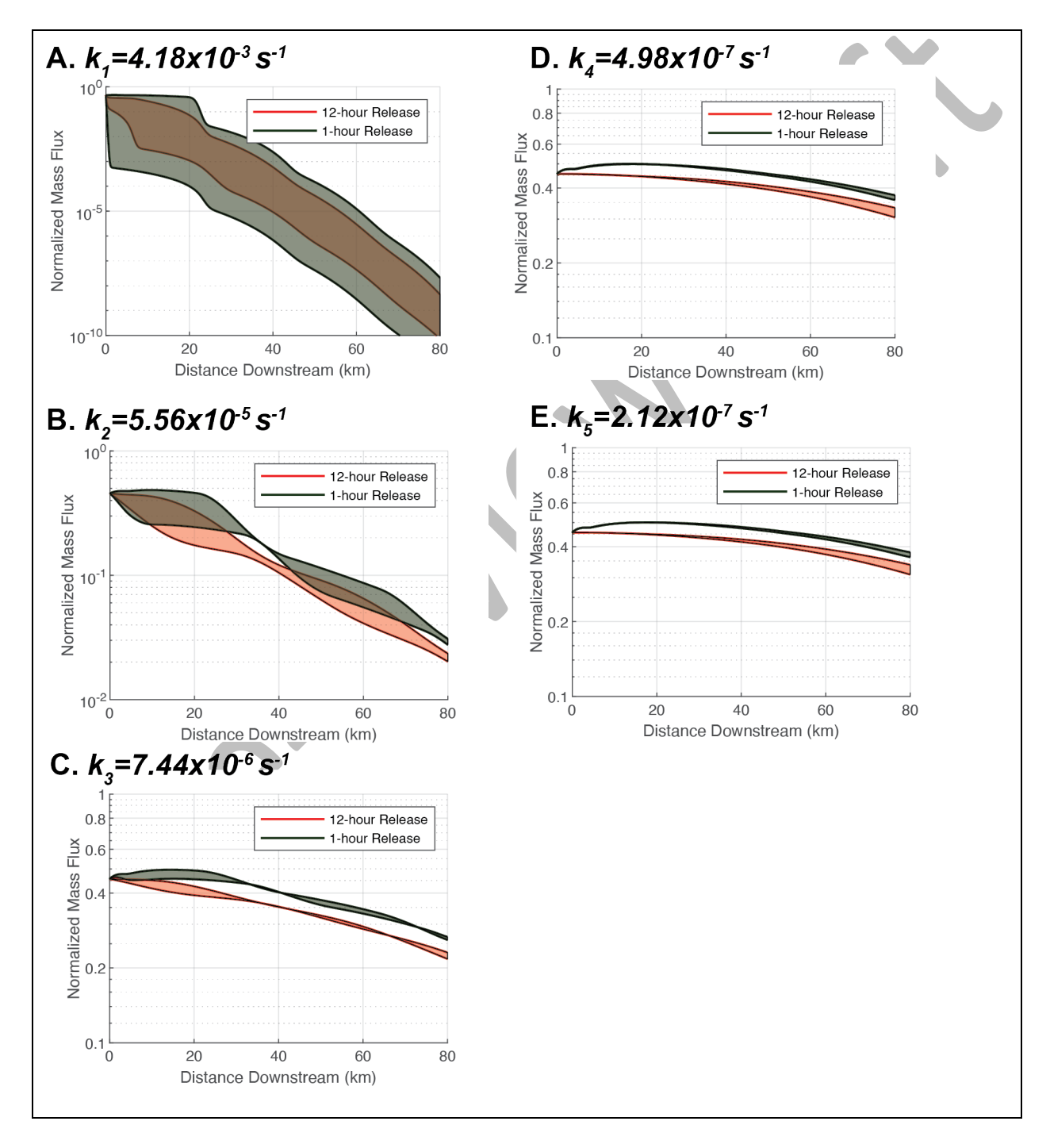


Figure 3. Impact of release timing and duration on the fraction of input mass passing each location along the simulated stream for 1-hr (green) and 12-hr (red) releases.

For k_1 , the range of exposures for 1 hr durations encompasses the range for 12 hr durations (Fig. 3a). The 12 hr exposures are partially (k_{2-3}) or entirely (k_{4-5}) below the range experienced for 1 hr injections for other reaction rates. For k_1 , release timing is the most dominant variable in determining downstream mass flux. As a result, short release durations could potentially be used to estimate the fate of longer release durations for compounds with fast photolysis rates.

Hyporheic zones are time-variable sources and sinks of mass to the stream, both limiting and exacerbating exposure depending on the location and time of interest (Fig. 4). Initially after the release begins, while there is no photolysis (advection after sunset), or the photolysis rate is low (k_{4-5}), concentration gradients result in mass being stored in the hyporheic zone where it is shielded from further photolysis. During peak photolysis, instream mass is rapidly removed and concentration gradients result in the net transfer of mass from the hyporheic zone into the stream. At the end of the photoperiod, high concentration "pulses" occur as mass that was previously stored in the hyporheic zone is returned to the stream each night. This results in downstream concentrations at either higher concentrations or above concentration thresholds for longer durations at downstream locations that those observed upstream (Fig. 4e-j).

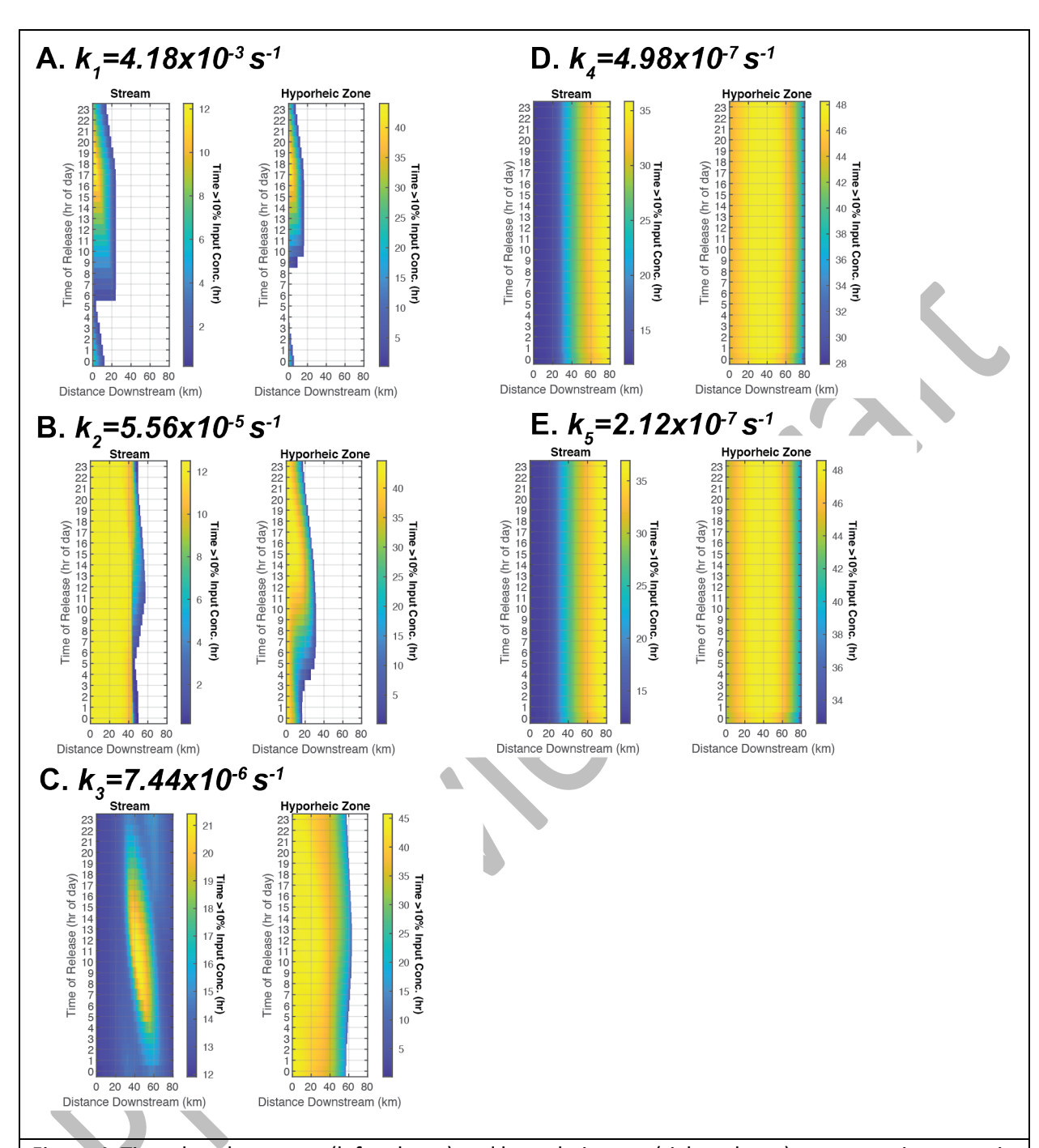


Figure 4. Time that the stream (left column) and hyporheic zone (right column) concentrations remain >10% of the input concentration (or 0.36 mg/L) for 12 hour release durations across varying release times, representing effective treatment for invasive sea lamprey. Rows are arranged from the fastest-to-slowest photolysis rate from top to bottom.

3.2 How do effective TFM treatment and TFM legacies vary with release time?

304

For the range of TFM photolysis rates (i.e., k_{2-4}), the first 20 km from the injection point is effectively treated regardless of injection timing (i.e., stream concentrations at or greater than 0.36 mg/L for 12 hours). Downstream from this point, treatment efficacy varies with photolysis rate as in-stream concentrations are dominated by photolysis (k_2) and storage in the hyporheic zone (k_{3-5} ; Fig. 4c, e, g). For k_2 , the maximum distance treated was about 42 km (for treatment beginning at 14:00; Fig. 4c). The impact of storage in the hyporheic zone can be best observed in (k_{3-4}). For these cases, high concentrations stored in the hyporheic zone during the 12-hr treatment act as a net source to the stream after the treatment has ended, resulting in in-stream treatment much than the designed 12-hr period (Fig. 4e, g). For k_{3-4} , about 20 km are treated regardless of release time, while downstream stream reaches are may ultimately maintain in-stream concentrations sufficient for treatment for more than 36-hr based on the designed 12-hr release.

Although TFM is expected to be rapidly removed from the tributaries of the Great Lakes through photolysis,³⁴ our recent work demonstrates photolysis removes less mass than indicated by early studies.^{37–39} Our simulations indicate extensive legacies of TFM in the stream and hyporheic zone should be expected (Fig. 4, right column). We find measurable stream and hyporheic concentrations should be expected for up to 48 hr after treatment ends (Fig. 4h). For k_2 , about 40 km of stream are effectively treated (Fig. 4c), but hyporheic locations near the injection site remain above the treatment threshold for more than three times as long as treatment requires. The maximum downstream distance of hyporheic zone treated is about 30 km for the release beginning at 09:00, with sensitivity in treatment distance as a function of release time (Fig. 4d).

As the photolysis rate decreases, other processes (e.g., transient storage, dispersion) grow in importance and a nonintuitive trend appears (Fig. 4e). For k_3 , the in-stream concentrations remain above 10% of the input concentration for 12 to 24 hr along the entire study reach. However, the longest duration occurs around 45 km downstream of the injection for release times beginning between 08:00 to 14:00 rather than near the injection site as might be expected. In this case, the increasing treatment duration up to 22 hours for stream reaches between 30-65 km downstream and mid-day injections is explained by mass stored in the hyporheic zone raising in-stream concentrations at night. Beyond the maximum duration at about 45 km, mass is increasingly photolyzed and dispersed such that the minimum threshold for treatment is not met. Put another way, interactions between hyporheic storage, photolysis, and advection in the absence of photolysis (at night) raise in-stream concentrations at specific, down-stream locations along the study reach.

For k_4 , treatment is achieved for the entire stream length across all injection timings (Fig 4g). Importantly, because photolysis is minimal for this case, downstream locations remain above the treatment threshold for substantially longer than is required for effective sea lamprey control. These extended timescales are attributable to TFM storage in hyporheic zones at the upstream end of the reach. The longest timescales of treatment in the hyporheic zone occur around 40 km downstream (Fig. 4h). This is due to the combination of (a) a relatively slow photolysis rate resulting in minimal removal during daylight hours, and (b) more upstream hyporheic zones to temporarily store and slowly release TFM.

Across all photolysis rates and injection timings simulated, at least some portions of the stream and hyporheic zone exceed concentrations and durations for the desired treatment (i.e., 1.1-1.4 times greater than the minimum lethal concentration) present for 2-4 times longer than the desired treatment of 12 hours. The extended treatment duration is a result of the steep concentration gradient between the stream and hyporheic zone near the release point causing high TFM concentrations to be stored in the hyporheic zone. This stored mass is slowly released over several days, resulting in elevated concentrations in the stream and downstream hyporheic zones well beyond the active treatment window. This phenomenon is particularly important in systems with relatively slow photolysis (k_{3-4}). These results indicate that modifying release times could tailor lampricide treatments based on stream reach and desired hyporheic treatment time. Moreover, results suggest that there is possible overtreatment occurring in some places and times in the river network, and that there is an opportunity for optimization of treatment practices.

4. Conclusions & Implications

Our primary objective was to advance our understanding of how time-variable reactivity and temporary storage of solutes in hyporheic zones interact to control the fate and transport of photolytic solutes in stream-hyporheic systems. For compounds with rapid photolysis rates (k_{1-2}), persistence varied by around 40 km in response to changes in release timing. Across all rates that represent TFM photolysis (k_{2-4}), persistence varied from <1 km to >80 km depending upon release time and the effective photolysis rate. For compounds with slow photolysis rates (e.g., carbamazepine, k_5) persistence was

independent of release timing. Similarly, in-stream concentrations and mass flux varied by several orders of magnitude as a function of release timing alone, with all other parameters held constant.

Release timing controls when, where, and for how long solute is stored in the hyporheic zone. For the rates simulated in this study, interactions between photolysis rate, hyporheic exchange, and stream transport are dominated by individual processes. Fate in systems with the fastest photolysis rates (k_1-k_2) is dominated by removal, while fate for reaches with slower photolysis rates (k_4-k_5) is dominated by transient storage and transport mechanisms, with minimal mass removal via photolysis. However, a moderate photolysis rate - representing the median reported TFM rate (k_3) - results in complex interactions of transport, removal, and storage processes, which produces complex behavior due to interactions between transport and transformation processes.

Shorter release durations have the greatest variability in persistence, in-stream concentrations, and mass flux as a function of release time. Less variation is observed as release duration increases, with a dynamic steady-state being achieved after about 48 hr of injection duration. These results highlight an opportunity to improve our predictive abilities and best management practices for photolytic compounds. For example, these findings could be operationalized to protect sensitive environments or drinking water intakes by adding consideration of release timing to the usual considerations of mass and concentrations being released.

The results of our study take the case of TFM as an example, given its widespread use and the risk of potential human and environmental risk. For TFM's fastest photolysis rate (k_2) , release times after peak photolysis require significantly lower input concentrations and retain mass in the system longer than early releases, while TFM's slowest photolysis rate (k_4) is insensitive to release timing. Of the 139 tributaries treated in 2015 and 2016, 98 tributaries had estimated photolysis rates the same order of magnitude as the fastest expected photolysis rate for TFM (k_2) . From these results, we expect modified timing and duration could be improved to reduce the mass required for treatment. Moreover, our simulations suggest the impacts and legacy of TFM application are less understood than previously thought. Indeed, we found the dynamic interactions of storage, transport, and transformation confound our predictive abilities. Finally, we underscore that our analysis here is limited to an idealized system. Still, we provide a framework to analyze the transport and fate of photolytic compounds which could be applied to a broad range of solutes and systems.

Acknowledgments:

This research was primarily supported by the Great Lakes Fishery Commission. Ward's time was additionally supported by DOE awards DE-SC0019377 and ORNL Mercury Science Focus Area and NSF award EAR-1652293. Data for this project are available on CUAHSI's HydroShare at http://www.hydroshare.org/resource/624b3e8641b94021887a4d824a9e1d53. Upon issuance of a DOI for this manuscript, the data will be assigned a corresponding DOI and available at https://doi.org/10.4211/hs.624b3e8641b94021887a4d824a9e1d53.

421 References:

- 422 (1) Hensley, R. T.; Cohen, M. J. On the Emergence of Diel Solute Signals in Flowing Waters. *Water Resour. Res.* **2016**, *52* (2), 759–772. https://doi.org/10.1002/2015WR017895.
- 424 (2) Blum, K. M.; Norström, S. H.; Golovko, O.; Grabic, R.; Järhult, J. D.; Koba, O.; Söderström
 425 Lindström, H. Removal of 30 Active Pharmaceutical Ingredients in Surface Water under Long426 Term Artificial UV Irradiation. *Chemosphere* **2017**, *176*, 175–182.
 427 https://doi.org/10.1016/j.chemosphere.2017.02.063.
- 428 (3) Lautz, L. K.; Fanelli, R. M. Seasonal Biogeochemical Hotspots in the Streambed around
 429 Restoration Structures. *Biogeochemistry* **2008**, *91* (1), 85–104. https://doi.org/10.1007/s10533430 008-9235-2.
- 431 (4) Von Gunten, H. R.; Karametaxas, G.; Krähenbühl, U.; Kuslys, M.; Giovanoli, R.; Hoehn, E.; Keil, R.
 432 Seasonal Biogeochemical Cycles in Riverborne Groundwater. *Geochim. Cosmochim. Acta* **1991**, *55*433 (12), 3597–3609. https://doi.org/10.1016/0016-7037(91)90058-D.
- Volkmar, E. C.; Henson, S. S.; Dahlgren, R. A.; O'Geen, A. T.; Van Nieuwenhuyse, E. E. Diel Patterns of Algae and Water Quality Constituents in the San Joaquin River, California, USA. *Chem.* Geol. **2011**, 283 (1–2), 56–67. https://doi.org/10.1016/j.chemgeo.2010.10.012.
- 437 (6) Kay, R. T.; Groschen, G. E.; Cygan, G.; Dupré David H., D. H. Diel Cycles in Dissolved Barium, Lead, 438 Iron, Vanadium, and Nitrite in a Stream Draining a Former Zinc Smelter Site near Hegeler, Illinois. 439 *Chem. Geol.* **2011**, *283* (1–2), 99–108. https://doi.org/10.1016/j.chemgeo.2010.10.009.
- Naftz, D. L.; Cederberg, J. R.; Krabbenhoft, D. P.; Beisner, K. R.; Whitehead, J.; Gardberg, J. Diurnal
 Trends in Methylmercury Concentration in a Wetland Adjacent to Great Salt Lake, Utah, USA.
 Chem. Geol. 2011, 283 (1–2), 78–86. https://doi.org/10.1016/j.chemgeo.2011.02.005.
- 443 (8) Gammons, C. H.; Babcock, J. N.; Parker, S. R.; Poulson, S. R. Diel Cycling and Stable Isotopes of
 444 Dissolved Oxygen, Dissolved Inorganic Carbon, and Nitrogenous Species in a Stream Receiving
 445 Treated Municipal Sewage. *Chem. Geol.* **2011**, *283* (1–2), 44–55.
 446 https://doi.org/10.1016/j.chemgeo.2010.07.006.
- 447 (9) Nimick, D. A.; Gammons, C. H.; Parker, S. R. Diel Biogeochemical Processes and Their Effect on 448 the Aqueous Chemistry of Streams: A Review. *Chem. Geol.* **2011**, *283* (1–2), 3–17. 449 https://doi.org/10.1016/j.chemgeo.2010.08.017.
- de Montety, V.; Martin, J. B.; Cohen, M. J.; Foster, C.; Kurz, M. J. Influence of Diel Biogeochemical Cycles on Carbonate Equilibrium in a Karst River. *Chem. Geol.* **2011**, *283* (1–2), 31–43. https://doi.org/10.1016/j.chemgeo.2010.12.025.
- 453 (11) Tobias, C.; Böhlke, J. K. Biological and Geochemical Controls on Diel Dissolved Inorganic Carbon
 454 Cycling in a Low-Order Agricultural Stream: Implications for Reach Scales and Beyond. *Chem.*455 *Geol.* **2011**, *283* (1–2), 18–30. https://doi.org/10.1016/j.chemgeo.2010.12.012.
- 456 (12) Carling, G. T.; Fernandez, D. P.; Rudd, A.; Pazmino, E.; Johnson, W. P. Trace Element Diel 457 Variations and Particulate Pulses in Perimeter Freshwater Wetlands of Great Salt Lake, Utah. 458 *Chem. Geol.* **2011**, *283* (1–2), 87–98. https://doi.org/10.1016/j.chemgeo.2011.01.001.
- 459 (13) Brown, G. W.; Krygier, J. T. Effects of Clear-Cutting on Stream Temperature. *Water Resour. Res.* 460 1970, 6 (4), 1133–1139. https://doi.org/10.1029/WR006i004p01133.

- 461 (14) Lowney, C. L. Stream Temperature Variation in Regulated Rivers: Evidence for a Spatial Pattern in Daily Minimum and Maximum Magnitudes. *Water Resour. Res.* **2000**, *36* (10), 2947–2955. https://doi.org/10.1029/2000wr900142.
- 464 (15) Nimick, D. A.; Gammons, C. H. Diel Biogeochemical Processes in Terrestrial Waters. *Chem. Geol.* **2011**, *283* (1–2), 1–2. https://doi.org/10.1016/j.chemgeo.2011.01.023.
- 466 (16) Ward, A. S.; Cwiertny, D. M.; Kolodziej, E. P.; Brehm, C. C. Coupled Reversion and Stream 467 Hyporheic Exchange Processes Increase Environmental Persistence of Trenbolone Metabolites.
 468 Nat. Commun. 2015, 6 (May), 7067. https://doi.org/10.1038/ncomms8067.
- Tixier, C.; Singer, H. P.; Canonica, S.; Müller, S. R. Phototransformation of Triclosan in Surface
 Waters: A Relevant Elimination Process for This Widely Used Biocide Laboratory Studies, Field
 Measurements, and Modeling. *Environ. Sci. Technol.* 2002, 36 (16), 3482–3489.
 https://doi.org/10.1021/es025647t.
- 473 (18) Brugger, A.; Slezak, D.; Obernosterer, I.; Herndl, G. J. Photolysis of Dimethyl Sulfide in Coastal
 474 Waters: Dependence on Substrate Concentration, Irradiance and DOC Concentration. *Mar.* 475 *Chem.* 1998, 59, 321–331.
- 476 (19) Toole, D. A.; Slezak, D.; Kiene, R. P.; Kieber, D. J.; Siegel, D. A. Effects of Solar Radiation on Dimethylsulfide Cycling in the Western Atlantic Ocean. *Deep. Res. Part I Oceanogr. Res. Pap.* 478 **2006**, *53* (1), 136–153. https://doi.org/10.1016/j.dsr.2005.09.003.
- 479 (20) Heffernan, J. B.; Cohen, M. J. Direct and Indirect Coupling of Primary Production and Diel Nitrate
 480 Dynamics in a Subtropical Spring-Fed River. *Limnol. Oceanogr.* 2010, 55 (2), 677–688.
 481 https://doi.org/10.4319/lo.2009.55.2.0677.
- 482 (21) Bencala, K. E.; Walters, R. a. Simulation of Solute Transport in a Mountain Pool-and-Riffle Stream:
 483 A Transient Storage Model. *Water Resour. Res.* **1983**, *19* (3), 718.
 484 https://doi.org/10.1029/WR019i003p00718.
- 485 (22) Brick, C. M.; Moore, J. N. Diel Variation of Trace Metals in the Upper Clark Fork River, Montana.
 486 Environ. Sci. Technol. 1996, 30 (6), 1953–1960. https://doi.org/10.1021/es9506465.
- 487 (23) Gammons, C. H.; Nimick, D. A.; Parker, S. R. Diel Cycling of Trace Elements in Streams Draining
 488 Mineralized Areas-A Review. *Appl. Geochemistry* 2015, *57*, 35–44.
 489 https://doi.org/10.1016/j.apgeochem.2014.05.008.
- 490 (24) Guillet, G.; Knapp, J. L. A.; Merel, S.; Cirpka, O. A.; Grathwohl, P.; Zwiener, C.; Schwientek, M. Fate
 491 of Wastewater Contaminants in Rivers: Using Conservative-Tracer Based Transfer Functions to
 492 Assess Reactive Transport. Sci. Total Environ. 2019, 656, 1250–1260.
 493 https://doi.org/10.1016/j.scitotenv.2018.11.379.
- 494 (25) Arrigoni, A. S.; Poole, G. C.; Mertes, L. A. K.; O'Daniel, S. J.; Woessner, W. W.; Thomas, S. A.
 495 Buffered, Lagged, or Cooled? Disentangling Hyporheic Influences on Temperature Cycles in
 496 Stream Channels. *Water Resour. Res.* **2008**, *44* (9), 1–13.
 497 https://doi.org/10.1029/2007WR006480.
- 498 (26) Poole, G. C.; O'Daniel, S. J.; Jones, K. L.; Woessner, W. W.; Bernhardt, E. S.; Helton, A. M.;
 499 Stanford, J. a.; Boer, B. R.; Beechie, T. J. Hydrologic Spiralling: The Role of Multiple Interactive
 500 Flow Paths in Stream Ecosystems. *River Res. Appl.* **2008**, *24*, 1018–1031.
 501 https://doi.org/10.1002/rra.

- 502 (27) Burkholder, B. K.; Grant, G. E.; Haggerty, R.; Khangaonkar, T.; Wampler, P. J. Influence of 503 Hyporheic Flow and Geomorphology on Temperature of a Large, Gravel-Bed River, Clackamas 504 River, Oregon, USA Barbara. *Hydrol. Process.* **2008**, *22*, 941–953. https://doi.org/10.1002/hyp.
- Ward, A. S.; Gooseff, M. N.; Voltz, T. J.; Fitzgerald, M.; Singha, K.; Zarnetske, J. P. How Does
 Rapidly Changing Discharge during Storm Events Affect Transient Storage and Channel Water
 Balance in a Headwater Mountain Stream? Water Resour. Res. 2013, 49 (9), 5473–5486.
 https://doi.org/10.1002/wrcr.20434.
- Schmadel, N. M.; Ward, A. S.; Kurz, M. J.; Fleckenstein, J. H.; Zarnetske, J. P.; Hannah, D. M.;
 Blume, T.; Vieweg, M.; Blaen, P. J.; Schmidt, C.; Knapp, J.; Klaar, M. J.; Romeijn, P.; Datry, T.;
 Keller, T.; Folegot, S.; Marruedo, A.; Krause, S. Stream Solute Tracer Timescales Changing with
 Discharge and Reach Length Confound Process Interpretation. *Water Resour. Res.* 2016, 50, 1–19.
 https://doi.org/10.1002/2015WR018062.Received.
- (30) Ward, A. S.; Schmadel, N. M.; Wondzell, S. M. Simulation of Dynamic Expansion, Contraction, and
 Connectivity in a Mountain Stream Network. Adv. Water Resour. 2018, 114, 64–82.
 https://doi.org/10.1016/j.advwatres.2018.01.018.
- Schmadel, N. M.; Ward, A. S.; Kurz, M. J.; Fleckenstein, J. H.; Zarnetske, J. P.; Hannah, D. M.;
 Blume, T.; Vieweg, M.; Blaen, P. J.; Schmidt, C.; Knapp, J.; Klaar, M. J.; Romeijn, P.; Datry, T.;
 Keller, T.; Folegot, S.; Marruedo, A.; Krause, S. Transport Timescales of Stream Solute Tracers
 Changing with Discharge and Reach Length Confound Process Interpretation. Water Resour. Res.
 2015, 51. https://doi.org/10.1002/2014WR016259.
- Vione, D.; Minero, C.; Maurino, V.; Pelizzettí, E.; Analitica, C.; Torino, U.; Giuria, V. Pietro.
 Seasonal and Water Column Trends of the Relative Role of Nitrate and Nitrite as OH Sources in
 Surface Waters. Ann. Chim. 2007, No. 97, 699–711.
- Yang, Z.; Hollebone, B. P.; Brown, C. E.; Yang, C.; Wang, Z.; Zhang, G.; Lambert, P.; Landriault, M.;
 Shah, K. The Photolytic Behavior of Diluted Bitumen in Simulated Seawater by Exposed to the
 Natural Sunlight. Fuel 2016, 186, 128–139. https://doi.org/10.1016/j.fuel.2016.08.068.
- 528 (34) Hubert, T. D. Environmental Fate and Effects of the Lampricide TFM: A Review. *J. Great Lakes Res.* **2003**, *29* (Supplement 1), 456–474. https://doi.org/10.1016/S0380-1330(03)70508-5.
- 530 (35) Gllderhus, P. A.; Johnson, B. G. H. Effects of Sea Lamprey (Petromyzon Marinus) Control in the 531 Great Lakes on Aquatic Plants, Invertebrates, and Amphibians. *Can. J. Fish. Aquat. Sci.* **1980**, *37* 532 (11), 1895–1905. https://doi.org/10.1139/f80-231.
- (36) Brege, D. C.; Davis, D. M.; Genovese, J. H.; McAuley, T. C.; Stephens, B. E.; Westman, R. W.;
 Wayne Westman, R. Factors Tesponsible for the Reduction in Quantity of the Lampricide, TFM,
 Applied Annually in Streams Tributary to the Great Lakes from 1979 to 1999. *J. Great Lakes Res.* 2003, 29 (Supplement 1), 500–509. https://doi.org/10.1016/S0380-1330(03)70511-5.
- 537 (37) McConville, M. B.; Hubert, T. D.; Remucal, C. K. Direct Photolysis Rates and Transformation
 538 Pathways of the Lampricides TFM and Niclosamide in Simulated Sunlight. *Environ. Sci. Technol.* 539 **2016**, acs.est.6b02607. https://doi.org/10.1021/acs.est.6b02607.
- (38) McConville, M. B.; Mezyk, S. P.; Remucal, C. K. Indirect Photodegradation of the Lampricides TFM and Niclosamide. *Environ. Sci. Process. Impacts* 2017, 19 (8), 1028–1039.
 https://doi.org/10.1039/c7em00208d.

543 (39)McConville, M. B.; Cohen, N. M.; Nowicki, S. M.; Lantz, S. R.; Hixson, J. L.; Ward, A. S.; Remucal, C. 544 K. A Field Analysis of Lampricide Photodegradation in Great Lakes Tributaries. Environ. Sci. Process. Impacts 2017, 00, 1-10. https://doi.org/10.1039/C7EM00173H. 545 546 (40)Runkel, R. L. One-Dimensional Transport with Inflow and Storage (OTIS): A Solute Transport 547 Model for Streams and Rivers; 1998. https://doi.org/Cited By (since 1996) 47\nExport Date 4 April 2012. 548 549 (41)Chapra, S. C. Surface Water-Quality Modeling; McGraw-Hill, 1997. Andreozzi, R.; Marotta, R.; Pinto, G.; Pollio, A. Carbamazepine in Water: Persistence in the 550 (42)551 Environment, Ozonation Treatment and Preliminary Assessment on Algal Toxicity. Water Res. 552 **2002**, 36 (11), 2869–2877. https://doi.org/10.1016/S0043-1354(01)00500-0. 553 (43)Matamoros, V.; Duhec, A.; Albaigés, J.; Bayona, J. M. Photodegradation of Carbamazepine, 554 Ibuprofen, Ketoprofen and 17α-Ethinylestradiol in Fresh and Seawater. Water. Air. Soil Pollut. 555 **2009**, 196 (1–4), 161–168. https://doi.org/10.1007/s11270-008-9765-1. 556 Service, U. S. F. and W.; Service, U. S. F. and W.; Oceans, D. of F. and. Top:012.5. 2015. (44)Potter, I. C. Ecology of Larval and Metamorphosing Lampreys. Can. J. Fish. Aquat. Sci. 1980, 37 557 (45)558 (11), 1641-1657. https://doi.org/10.1139/f80-212. Johnson, N. S.; Twohey, M. B.; Miehls, S. M.; Cwalinski, T. A.; Godby, N. A.; Lochet, A.; Slade, J. 559 560 W.; Jubar, A. K.; Siefkes, M. J. Evidence That Sea Lampreys (Petromyzon Marinus) Complete Their Life Cycle within a Tributary of the Laurentian Great Lakes by Parasitizing Fishes in Inland Lakes. J. 561 Great Lakes Res. 2016, 42 (1), 90-98. https://doi.org/10.1016/j.jglr.2015.10.011. 562